RNA (1997), 3:748–763. Cambridge University Press. Printed in the USA.

Mutational analysis of the protein subunits of the signal recognition particle Alu-domain

NAZARENA BUI,[1] NICOLE WOLFF,[2] STEPHEN CUSACK,[2] and KATHARINA STRUB[1]

[1]Département de biologie cellulaire, Université de Genève, Sciences III, CH-1211 Geneva 4, Switzerland
[2]European Molecular Biology Laboratory (EMBL), Grenoble Outstation, c/o I.L.L.156X, 38042 Grenoble Cedex 9, France

ABSTRACT

Two polypeptides of the murine signal recognition particle (SRP), SRP9 and SRP14, bind exclusively as a heterodimer to SRP RNA and their presence is required for elongation arrest activity of the particle. SRP9/14 also constitute a subunit of small cytoplasmic Alu RNPs. To identify RNA-binding determinants, we assayed the dimerization and RNA-binding capacities of altered proteins in vitro. Despite the structural homology of the two proteins, their requirements for dimerization differ substantially. In SRP9, an internal fragment of 43 amino acids is sufficient to allow dimer formation, whereas in SRP14 only few changes, such as removing an internal loop region, are tolerated without affecting its dimerization activity. The dimerization defect of the SRP14 proteins is most likely explained by a reduced stability or ability to fold of the proteins. Interestingly, SRP RNA can engage certain dimerization-defective SRP14 proteins into stable complexes, suggesting that low-affinity interactions between the RNA and SRP14 may help to overcome the folding defect or the reduced stability of the proteins. We identified two regions, one in each protein, that are essential for RNA-binding. In SRP9, acidic amino acid residues in the N-terminal α-helix and the adjacent loop and, in SRP14, a flexible internal loop region are critical for RNA-binding. In the heterodimer, the two regions are located in close proximity, consistent with the RNA-binding region being formed by both proteins.

Keywords: Alu RNA; dimerization; RNA–protein; SRP9; SRP14

INTRODUCTION

The signal recognition particle (SRP) plays an essential role in the translocation of proteins into the endoplasmic reticulum. It mediates co-translational translocation by recognizing and binding to signal sequences of nascent chains followed by targeting the nascent chain-ribosome complex to the translocation sites in the ER membrane (for review see Walter & Johnson, 1994; Bovia & Strub, 1996; Walter & Johnson, 1994). The components as well as the functions of canine SRP have already been characterized quite well (for review see Lütcke, 1995; Bovia & Strub, 1996). SRP is composed of six polypeptides and one RNA molecule. The 54-kDa subunit of SRP (SRP54) binds specifically to the signal sequence of a nascent chain and, together with the 19-kDa subunit (SRP19) and SRP RNA, promotes targeting and translocation of elongation-arrested nascent chains (Hauser et al., 1995). The targeting cycle of SRP is regulated by GTP-binding and hydrolysis reactions of SRP54 and of the SRP receptor complex in the endoplasmic reticulum membrane (Rapiejko & Gilmore, 1992; Miller et al., 1993; Bacher et al., 1996). While SRP is bound to the nascent chain-ribosome complex, it effects a delay or an arrest in the elongation of the nascent polypeptide. The delay in elongation is thought to improve the efficiency of the translocation. The 9-kDa and 14-kDa subunits of SRP (SRP9, SRP14) and the Alu sequences of SRP RNA are required for elongation arrest activity of the particle (Siegel & Walter, 1986; for review see Strub et al., 1993). Homologues of SRP components have been identified in organisms of all three kingdoms, indicating that SRP-mediated protein translocation is highly conserved in evolution (for review see Althoff et al., 1994; Wolin, 1994). Indeed, functional studies in yeast and bacteria corroborated this conclusion (Hann et al., 1989; Luirink et al., 1992; Phillips & Silhavy, 1992).

The Alu sequences of mammalian SRP RNA constitute the phylogenetic precursor for the Alu family of repetitive DNA sequences in primate and rodent genomes (Ullu & Tschudi, 1984). Recently, it has been shown for a number of cytoplasmic Alu RNAs that

Reprint requests to: Katharina Strub, Département de biologie cellulaire, Université de Genève, Sciences III, Ch-1211 Geneva 4, Switzerland; e-mail: strub@cellbio.unige.ch.

they can bind SRP9/14 in vivo and in vitro (for review see Bovia & Strub, 1996). In addition, SRP9/14 was found to exist in large excess over SRP in primate cells (Chang & Maraia, 1993; Chang et al., 1994; Bovia et al., 1995). Although no functions have yet been identified for Alu RNPs and the free heterodimer, it appears likely that the heterodimer SRP9/14 may have additional, not SRP-related cellular functions.

SRP9 and SRP14 form a very stable heterodimer in vitro and bind exclusively as such with high specificity to the Alu portion of mammalian SRP RNAs (Strub & Walter, 1990) and to scAlu RNAs (Bovia et al., 1995, 1997). The dissociation constants for mammalian SRP9/14 heterodimers and a synthetic mammalian SRP RNA are in the range of 0.08–0.2 nM (Janiak et al., 1992; Bovia et al., 1997), demonstrating that these RNA–protein complexes are exceptionally stable.

The primary sequences of mouse SRP9 and SRP14 proteins failed to reveal already characterized RNA-binding motifs. We therefore decided to use mutagenesis, followed by functional assays, to identify structural elements within the two polypeptides that are essential for the formation of the heterodimer and for binding to the Alu-portion of SRP RNA. In molecular terms, dimerization may bring distinct regions in both proteins in close proximity, thereby forming an RNA-binding pocket. Alternatively, the RNA-binding domain may consist of only one protein and could be generated by conformational changes during dimerization. Our analysis demonstrated that both subunits of the heterodimer SRP9/14 contribute to the formation of the RNA-binding domain. Based on the crystal structure of the heterodimer, which was determined in parallel (Birse et al., 1997), the RNA-binding determinants are located in the N-terminal α-helix and the following turn of SRP9 and in a flexible loop region of SRP14. Despite the structural similarity between SRP9 and SRP14 and the symmetry of the heterodimer, changes in the primary structures of the two proteins affect their dimerization capacities very differentially. Whereas an internal fragment of SRP9 is sufficient to promote dimerization, only few changes in SRP14 are tolerated without losing its dimer formation capacity, indicating that most of the changes interfere with its folding or stability. Certain SRP14 proteins with a defective dimerization function formed in the presence of SRP9 stable complexes with SRP RNA, suggesting that low-affinity interactions between the RNA and the proteins can drive the assembly of the complex.

RESULTS

Experimental strategy

To determine structural elements within murine SRP9 and SRP14 that are required for the formation of the SRP9/14–SRP RNA complex, we engineered SRP9 and SRP14 proteins with N- and C-terminal truncations. The secondary structure arrangement of the proteins (Birse et al., 1997) and a schematic representation of the truncated proteins that we obtained by introducing deletions into the SRP9 and SRP14 cDNAs (see Materials and Methods) are shown in Figure 1A and B. We also produced a series of SRP14 proteins in which two adjacent amino acids were substituted by introducing a restriction site at this position into the SRP14 cDNA. In these SRP14 proteins, many of the conserved amino acids in the central region of SRP14, in particular basic amino acids, were replaced by either A/S or A/G (Fig. 1C). In addition, the newly introduced restrictions sites served to produce internal deletions in the SRP14 cDNA (labeled * in Fig. 1B). Hence, the two amino acids that precede the internal truncations in these proteins have been changed into alanine and serine.

SRP9 and SRP14 have to form a heterodimer to bind specifically to SRP RNA (Strub & Walter, 1990). Hence, we first determined the dimerization capacities of the altered SRP9 and SRP14 proteins using three different approaches in which co-precipitation of the altered protein with its partner protein revealed its capacity to form a heterodimer. For the analysis of SRP9 proteins, we used affinity-purified anti-SRP14 antibodies to co-precipitate SRP9 proteins with purified recombinant SRP14, which contains a myc epitope at its C-terminus (SRP14m). As an alternative, we produced a fusion protein of SRP14 with glutathione-S-transferase (G-14). The glutathione-S-transferase (GST) moiety of the fusion protein serves to bind the protein to glutathione beads, which allows easy separation of bound and free SRP9 proteins (see Materials and Methods). The dimerization capacities of SRP14 proteins were examined in co-precipitation experiments with recombinant SRP9 comprising a myc epitope at its C-terminus (SRP9m) and immobilized anti-myc antibodies.

In trial experiments, we found that salt concentrations between 150 and 500 mM potassium acetate did not influence the efficiency of dimer formation. In addition, dimerization was as efficient co-translationally—when one protein was present during in vitro synthesis of the other—as posttranslationally—when the recombinant partner protein was combined with the fully synthesized [^{35}S]-labeled protein (results not shown). In all experiments presented here, the recombinant proteins were added posttranslationally in an estimated 10-fold excess to the in vitro synthesized [^{35}S]-labeled proteins. It should be noticed that a loss in dimerization capacity in these experiments can reflect a loss in direct interactions between the two proteins or result from aberrant folding of the mutated protein.

To assay the RNA-binding activity of the heterodimer, we used biotinylated 7S-Alu RNA and, as a negative control, a biotinylated transcript representing a portion of the antisense strand of the murine SRP14

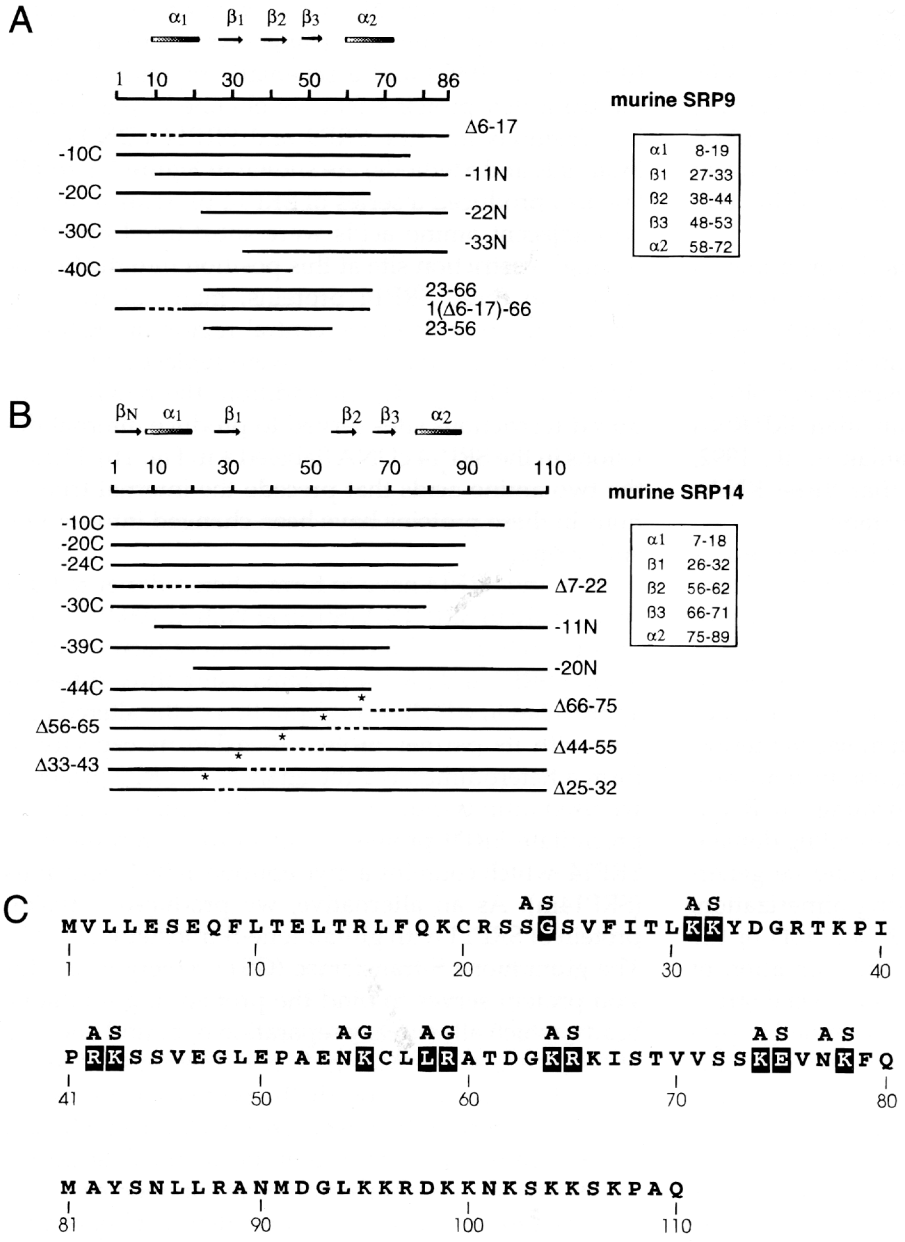

FIGURE 1. Schematic representation of the mutations introduced into SRP9 and SRP14 proteins. **A:** Murine SRP9. **B:** Murine SRP14. Dashed lines designate removed regions. * indicates that the two amino acids preceding the truncated region have been changed into alanine and serine. The α-helices and β-strands in both proteins are indicated according to Birse et al. (1997). The boundaries of the secondary structures are shown to the left. **C:** Substitution of a amino acid residues in SRP14. Black: Highly conserved amino acid residues based on the alignment of the SRP14 proteins of *Mus musculus*, *A. thaliana*, *O. sativa* (N. Bui, N. Wolff, & K. Strub, unpubl. results, accession no: Y 10 116, Y 10 117) and *S. cerevisiae* (Brown et al., 1994). Only the conservation of the mutated residues is shown. The overall conservation of the proteins as compared to the murine protein are 50% (*A. thal*), 40% (*O. sat.*) and 30% (*S. cer.*).

cDNA. We have shown previously that the negative control RNA is not bound by murine SRP9/14 (Bovia et al., 1994). Studies conducted in parallel demonstrated that the murine SRP9/14-synthetic 7S-Alu RNA complex is very stable, with a dissociation constant of 0.2 nM (Bovia et al., 1997). The same quantitative study also revealed that a 10–15-fold decrease in the dissociation constant of the complex was not detected by the in vitro RNA-binding assay. The concentrations of the [^{35}S]-labeled proteins are significantly above 0.2 nM (5–10 nM), which may explain this observation. Hence, a loss in RNA-binding activity in this assay reflects a 20-fold or larger decrease in the binding constant of the complex.

A central region of SRP9 is required and sufficient for the formation of a heterodimer

The polyclonal anti-SRP14 antibodies co-precipitated wild-type SRP9 with an efficiency of about 40% (Fig. 2A, lane 1), whereas SRP9 bound with 26% efficiency to glutathione beads in the presence of G-14 (Fig. 2B, lane 1). The input lanes represent either all of the SRP9 protein (Fig. 2, I) or 1/3 of the protein (Fig. 2, $I_{1/3}$) used in the dimerization reaction. In the absence of SRP14m, about 10% of the labeled SRP9 protein was nonspecifically co-precipitated with the polyclonal antibodies (Fig. 2A, lane 3). When G-14 was replaced by GST (Fig. 2B, lane 3), nonspecific binding of SRP9 to glutathione beads was not detectable. For the calcula-

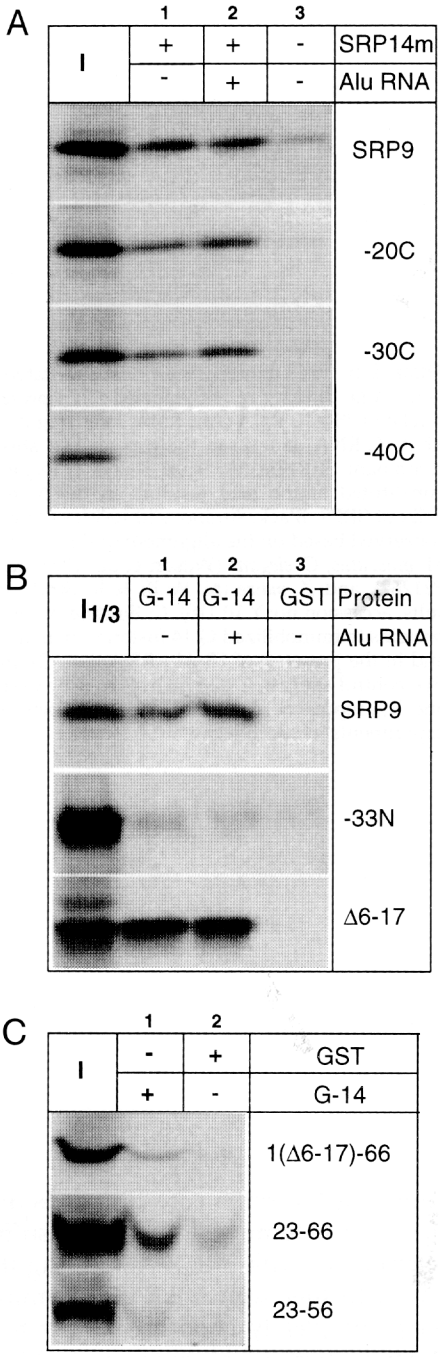

FIGURE 2. Dimerization capacities of truncated SRP9 proteins. **A:** Co-immunoprecipitation of [^{35}S]-labeled SRP9 proteins with affinity-purified anti-SRP14 antibodies in the presence (lane 1,2) and in the absence (lane 3) of recombinant SRP14m and 7S-Alu RNA. **B,C:** Binding of [^{35}S]-labeled SRP9 proteins to immobilized recombinant G-14 fusion protein alone (lane 1) and in the presence of 7S-Alu RNA (lane 2 in B). In the negtive control sample, G-14 was replaced by GST (B: lane 3; C: lane 2). I and $I_{1/3}$ represent all and 1/3 of the protein used in the experiments, respectively.

tion of the dimerization capacities of the truncated SRP9 proteins, nonspecific binding in the control lane was deduced from specific binding in the experimental samples. The co-precipitation efficiencies of the truncated SRP9 proteins were then standardized to the co-precipitation efficiency of wild-type SRP9, which was set to 100% (Table 1A).

Truncation of C-terminal portions up to 30 amino acids and of an internal portion at the N-terminus, amino acids 6–17, which remove the N- and C-terminal α-helices (Fig. 1A), did not interfere significantly with the formation of a heterodimer (Table 1A). When removing similar N-terminal portions completely, as in SRP9-11N and SRP9-22N, we still observed dimerization, however, at 2–3-fold lower efficiencies. Possibly, the complete removal of N-terminal portions resulted in a more severe disturbance of the SRP9 structure than the removal of the α1-helix. Removing 33 and 40 amino acids at the N and C termini, respectively, completely abolished heterodimer formation (Fig. 2A,B, lane 1).

We also determined the dimerization efficiencies of the truncated proteins in the presence of 7S-Alu RNA to reveal a potential role of the RNA in dimer stability or assembly. The heterodimer SRP9/14m and SRP9/G-14 bound with similar efficiencies to 7S-Alu RNA (Fig. 3B and results not shown), as determined previously for SRP9/14 (Bovia et al., 1994). No difference in dimerization capacity with and without 7S-Alu RNA was observed for wild-type SRP9 (Fig. 2A, lane 2).

TABLE 1. Dimerization and RNA-binding efficiencies of SRP9 proteins.[a]

	Dimerization		RNA-binding	
SRP9 proteins	− Alu RNA	+ Alu RNA	Alu RNA	C RNA
A. SRP9 proteins with truncations				
SRP9 (1–86)	100	100	100	13
1–76 (–10C)	110	119	++[b]	—[c]
1–66 (–20C)	80	94	121	20
1–56 (–30C)	81	100	83	13
1–46 (–40C)	11	—	—	—
12–86 (–11N)	44	50	26	—
23–86 (–22N)	39	33	11	13
34–86 (–33N)	—	—	—	—
(Δ6–17)[d]	131	123	13	9
1(Δ6–17)–66[e]	11	13	ND	ND
23–66[e]	14	11	ND	ND
23–56	—	—	ND	ND
B. SRP9 proteins with mutations in the terminal part				
W7A, E8G[f]	59	87	87	—
E9A, F10G	31	24	38	12
R12A, A13G	78	65	86	—
E15G[d]	108	111	49	—
K16A, L17G	19	11	42	—
D21A, P22G[d]	128	98	45	—

[a] Activities of mutated proteins were standardized to 100% dimerization and RNA-binding efficiencies of wild-type SRP9. Standard deviations in the experimental approaches were between 10 and 20%. ND, not determined.
[b] Previously published without quantification in Bovia et al. (1994).
[c] Less than 10% binding.
[d] Specific loss of RNA binding.
[e] Minimal region for dimerization.
[f] Improved dimerization efficiency in presence of the RNA.

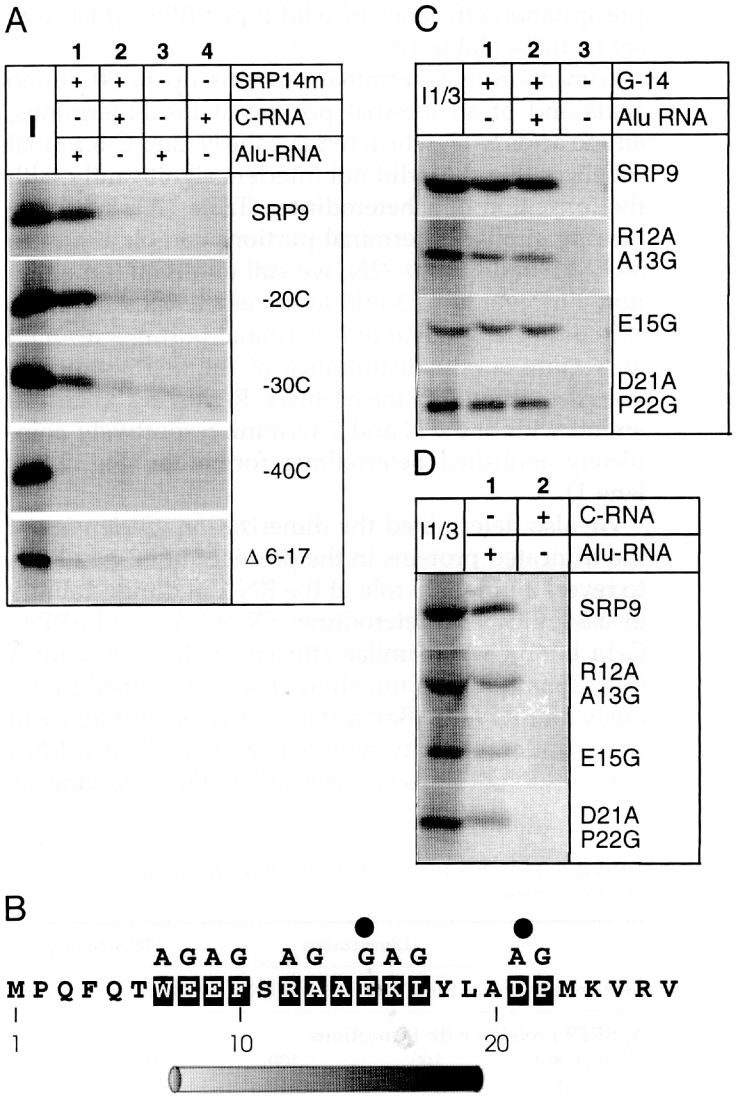

FIGURE 3. RNA-binding activities of mutated SRP9 proteins. **A,D:** Binding of [^{35}S]-labeled SRP9 proteins to biotinylated 7S-Alu RNA (Alu RNA, lane 1) and to a control RNA (C-RNA, lane 2) in the presence or absence of recombinant SRP14m (A: lanes 3 and 4, respectively). **B:** Substituted amino acid residues in the N-terminal α1-helix of SRP9. Black: Amino acid residues that are highly conserved based on the alignment of the SRP9 proteins of *M. musculus*, *C. elegans* (Wilson et al., 1994, accession no: P21262), and *Z. maize* (N. Wolff & K. Strub, unpubl. results, accession no: Y 10 118). **C:** Binding of mutated SRP9 proteins to immobilized G-14 fusion protein alone (lane 1) and in the presence of 7S-Alu RNA (lane 2). In the negative control sample, G-14 was replaced by GST (lane 3). I and $I_{1/3}$ represent all and 1/3 of the protein used in the experiments, respectively.

This confirmed that binding of SRP9 to SRP14m and G-14 is maximal under the selected experimental conditions. The dimerization capacities of C-terminally truncated proteins were increased slightly, indicating that the RNA stabilized the complex (Fig. 2A, lane 2). In contrast, the addition of 7S-Alu RNA did not improve the reduced dimerization capacity of N-terminally truncated SRP9 proteins, suggesting that they may be defective in RNA binding.

The finding that certain N- and C-terminal regions may be removed individually without a complete loss of the dimerization function indicated that a central region of about 45–50 amino acids of SRP9 may be sufficient to form a heterodimer with SRP14 in vitro. To confirm this interpretation, we examined dimer formation of internal portions of SRP9 (Figs. 1A, 2C). An SRP9 protein comprising amino acids 23–66 and SRP9(1(Δ6–17)–66) were both found to form a heterodimer with SRP14m, albeit less efficiently than SRP9 (Fig. 2C, lane 1; Table 1A). Thus, the central region of SRP9 comprising the three core β-strands and more than half of the C-terminal α2-helix is sufficient to form a heterodimer with SRP14. Removing the entire α2-helix by a further truncation of 10 amino acids, SRP9(23–56), completely abolished dimer formation. Hence, removing both α-helices (α1 and α2 in Fig. 1A) is detrimental for dimer formation, whereas removing either α1 (SRP9(Δ6–17) or α2 (SRP9-30C) leaves the protein dimerization-competent. This findings suggest that the α-helices play an important role in stabilizing the structure of the central β strands to allow dimer formation.

The N-terminal region of SRP9 contains RNA-binding determinants

We then examined the RNA-binding activities of the heterodimeric complexes comprising SRP14m and the truncated in vitro-synthesized SRP9 proteins (Fig. 3A, lane 1). About 40% of the in vitro-synthesized SRP9

protein bound to 7S-Alu RNA and less than 4% bound to the negative control RNA (lane 2). Instead of subtracting nonspecific from specific RNA-binding, we decided to list them separately, because mutations in the protein could change its RNA-binding specificity. In addition, we standardized the RNA-binding efficiencies of the altered proteins to the one of SRP9/14 bound to 7S-Alu RNA (Table 1).

We found that removing up to 30 amino acids at the C terminus of SRP9 did not interfere with RNA binding of the heterodimer (Fig. 2A, lane 1). Hence, this region is dispensable for dimer formation and RNA-binding activities of SRP9. In contrast, N-terminally truncated proteins, in particular SRP9(Δ6–17), which dimerized as efficiently as wild-type SRP9, failed to bind specifically to 7S-Alu RNA (Fig. 3A, lane 1; Table 1A). The two proteins that did not form a heterodimer, SRP9-40C and SRP9-33N, were also defective in 7S-Alu RNA-binding. The two negative controls, binding of truncated SRP9 proteins alone to 7S-Alu RNA, and binding of the heterodimer to a control RNA gave the expected negative results, thereby confirming that the RNA-binding activity of the mutated proteins was still dependent on heterodimer formation (Fig. 3A).

The intact dimerization function of SRP9(Δ6–17) strongly indicated that its complete loss in RNA-binding activity is due to a loss of an RNA-binding domain as opposed to a change in protein structure. To confirm this interpretation and to identify specific amino acid residues involved in RNA-binding, we replaced one or two adjacent amino acids by A and G within this region of SRP9 (Fig. 3B). We were hoping that the newly introduced alanine and glycine residues would not interfere significantly with the formation of an α-helix. As before, the proteins were produced in wheat germ extract and their dimerization and RNA-binding activities assayed with immobilized G-14 and 7S-Alu RNA, respectively (Fig. 3C,D, lane 1; Table 1B). The mutations that reduced the RNA-binding activity of the protein exclusively, but left its dimerization capacity unchanged, are E15G and D21A/P22G. E15 is located in the α1-helix and D21 and P22 in the following turn (Fig. 1A). W7A/E8G had a reduced dimerization capacity, but formed a stable complex with the RNA, revealing an intact RNA-binding function of the heterodimer. Mutations such as K16A/L17G and E9A/F10G had a negative effect on dimerization and RNA-binding activities of the protein. The fact that the dimerization defect was not compensated by the addition of the RNA, as observed for SRP9(W7A/E8G), suggests that these residues play a role in RNA binding. The mutation of R12A/A13G did not diminish both activities. The negative control reactions in the experiments—binding of the heterodimer to the control RNA (Fig. 3D, lane 2) and binding of the altered SRP9 proteins alone to both RNAs (not shown)—gave similar results as observed for SRP9. The specific negative effect of certain substitutions on the RNA-binding function of the heterodimer confirmed the importance of this region, and, in particular, of these residues, for RNA-binding.

An internal loop and a small C-terminal region can be removed in SRP14 without interfering with its dimerization capacity

Next, we analyzed truncated SRP14 proteins and proteins with one or two adjacent amino acid substitutions for their capacity to form a heterodimer (Fig. 1B,C). The similarity of SRP14 and SRP9 structures (Birse et al., 1997; Fig. 1B) suggested that similar truncations in SRP14 might yield results comparable to the ones obtained for SRP9.

Under optimized conditions, 22% of the wild-type in vitro synthesized SRP14 protein was specifically coprecipitated with anti-myc antibodies in the presence of SRP9m (Fig. 4A, lane 1, Table 2). Very little SRP14, below 3% of the protein used in the experiment, was precipitated in the negative control where SRP9m was omitted from the immunoprecipitation reaction (Fig. 4A,B). The dimerization capacities of the altered SRP14 proteins were calculated as mentioned for SRP9 proteins.

Three regions in SRP14 were found to be dispensable for dimer formation; the 10 C-terminal amino acids and the internal regions spanning amino acids 33–43 and 44–55, which represent a flexible loop structure in the SRP14 protein (Fig. 1B). Removal of other internal regions, as well as N-terminal regions and 20 or more amino acids C-terminally, resulted in a complete loss of dimerization activity. Because not all of these regions are part of the dimer interface (see Discussion), these results suggested that SRP14, unlike SRP9, requires a largely intact protein sequence for its correct folding. Indeed, for many of the truncated proteins that lacked dimerization activity, we observed a noticeable increase in nonspecific co-immunoprecipitation (for example, for the internal truncation Δ56–66 in Fig. 4B). We think that this is due to aberrant folding of these proteins, which renders them either partially insoluble and/or very sticky.

In contrast to the truncated proteins, all but one of the SRP14 proteins with amino acid substitutions had full dimerization capacities (Fig. 4B, lane 1; Table 2). Hence, the replaced amino acids are not critical for dimerization. Substitution of amino acids L58 and R59 (Fig. 4B; Table 2) as well as other changes in the vicinity (results not shown) resulted in a decreased dimerization efficiency. Thus, subtle changes in primary sequence within this core region appears to diminish the stability of the heterodimeric complex and/or to interfere with proper folding of the SRP14 protein.

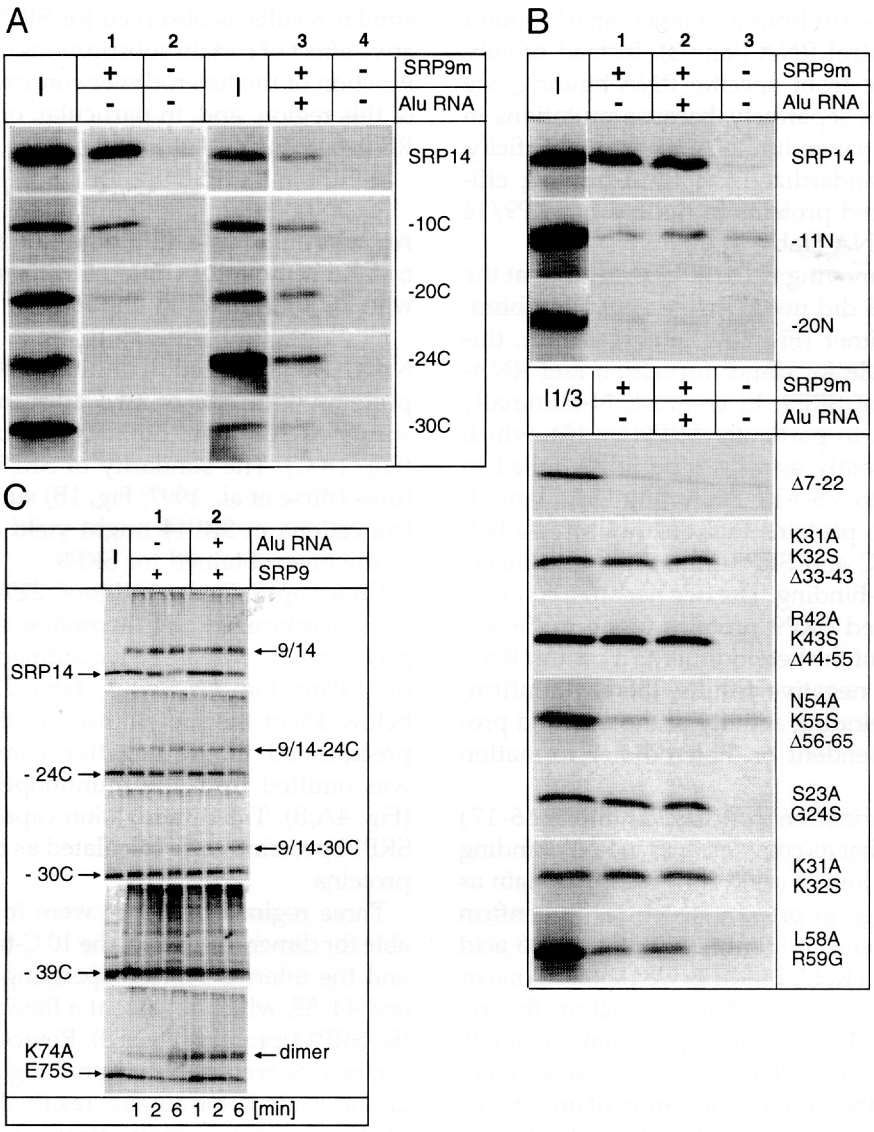

FIGURE 4. Dimerization activities of altered SRP14 proteins. **A,B:** Co-immunoprecipitation of [^{35}S]-labeled SRP14 proteins with anti-myc antibodies in the presence of SRP9m (A: lane 1; B: lane 1) and in the presence of SRP9m and 7S-Alu RNA (A: lane 3; B: lane 2). SRP9m was omitted in the negative control reaction (A: lanes 2,4; B: lane 3). **C:** Glutaraldehyde-mediated crosslinking of SRP9 and SRP14 proteins in the heterodimer in the presence (lane 2) and in the absence (lane 1) of 7S-Alu RNA. [^{35}S]-labeled SRP14 proteins were crosslinked to recombinant SRP9 for the time length indicated. I and $I_{1/3}$ represent all and 1/3 of the protein used in the experiments, respectively.

We also determined the dimerization efficiencies of the various SRP14 proteins in the presence of 7S-Alu RNA (Fig. 4A, lane 2; Fig. 4B, lane 3; Table 2). The dimerization capacity of wild-type SRP14 remained the same in the presence of the RNA, confirming that the selected experimental conditions were optimal for dimerization. The lost dimerization capacities of N-terminally and internally truncated proteins were not improved in the presence of 7S-Alu RNA. A significant RNA-dependent increase in dimerization efficiency was observed for SRP14-20C and, surprisingly, also for SRP14-24C and SRP14-30C, for which we failed to detect dimeric complexes in the absence of 7S-Alu RNA (Fig. 4A, lane 3; Table 2). To examine whether these complexes were present in solution but escaped detection in immunoprecipitation experiments, we took advantage of the divalent crosslinking reagent glutaraldehyde, which has been shown previously to crosslink SRP9 and SRP14 proteins efficiently in solution (Strub & Walter, 1990; Bovia et al., 1994). For these experiments, the [^{35}S]-labeled translation products were purified partially on heparin beads and then incubated with recombinant SRP9, with or without 7S-Alu RNA. Glutaraldehyde was added to the samples and crosslinking stopped at different time points. We observed a crosslinked product of the expected size for SRP14-24C, -30C and SRP14 (K74A, E75S) (Fig. 4C; Table 2). As observed previously for wild-type SRP9/14

(Strub & Walter, 1990; Bovia et al., 1994), these crosslinked products were specific for the heterodimer, because they were not detected in the absence of recombinant SRP9 (results not shown). The crosslinking efficiencies were similar with and without 7S-Alu RNA for SRP14 and SRP14-24C, whereas they improved in the presence of the RNA for SRP9/14-30C and for SRP14 (K74A, E75S). The fact that certain complexes were observed in crosslinking but not in immunoprecipitation experiments indicated that they have a decreased stability and that the addition of the RNA moiety helped to improve it. Hence, missing or altered amino acids in the C-terminal region have no significant role in RNA binding, but stabilize the heterodimeric complex. We failed to detect a crosslinked product between SRP14-39C and SRP9, suggesting that the truncated protein has lost both activities.

RNA-binding determinants of SRP14 are located within a flexible loop region

We next examined the RNA-binding activities of the mutated SRP14 proteins (Fig. 5A,B, lane 1; Table 2). We have shown previously that the RNA-binding activity of SRP14-10C is the same as for SRP14 (Bovia et al., 1994). Of the other two truncated proteins that dimerized efficiently, one, SRP14 (R42A, K43S, Δ44-55), had wild-type RNA-binding activity, whereas the other, SRP14 (K31A, K32S, Δ33-43), had a significantly decreased RNA-binding activity, indicating that amino acid residues 31-43 are required for RNA binding. The results obtained with the other truncated SRP14 proteins were as expected from the observed effect of 7S-Alu RNA on heterodimer stability. The C-terminally truncated proteins that lack up to 24 amino acids still bound to 7S-Alu RNA with the same efficiency as SRP14. Removing 30 amino acids C-terminally decreased RNA-binding and dimerization activities to 55%. The N-terminally truncated proteins, as well as the proteins with internal truncations that had lost their capacities for dimer formation, had also completely lost their RNA-binding activities (Table 2). The specific RNA-binding activity observed for certain SRP14 proteins was strictly dependent on the presence of SRP9 (not shown). Some of the SRP14 proteins, such as SRP14 (N54A, K55S, Δ56-65), that co-precipitated nonspecifically in the immunoprecipitation experiments, also showed an increased nonspecific binding to the control RNA, suggesting stickiness and/or insolubility of the proteins. The slight increase in binding to the control RNA observed for the C-terminally truncated proteins may indeed reflect an increased nonspecific affinity for RNA.

TABLE 2. Dimerization and RNA-binding efficiencies of SRP14 proteins.[a]

	Dimerization		RNA-binding	
Proteins	− Alu RNA	+ Alu RNA	Alu RNA	C RNA
SRP14 (1-100)	100	100	100	11
1-100 (-10C)[b]	103	124	++[c]	32
1-90 (-20C)[d]	21	98	109	25
1-86 (-24C)[d]	−(+)[e]	83	95	17
1-80 (-30C)[d]	−(+)[e]	62	55	17
1-71 (-39C)	—	—	—	—
1-65 (-44C)	—	—	—	—
12-110 (-11N)	—	—	—	—
21-110 (-20N)	—	—	—	—
Δ(7-22)	—	—	—	—
S23A, G24S	100	111	97	10
S23A, G24S (Δ25-32)	16	—	16	13
K31A, K32S	119	115	103	—
K31A, K32S (Δ33-43)[b,f]	82	87	37	10
R42A, K43S	72	109	94	10
R42A, K43S (Δ44-55)[b]	106	106	100	—
N54A, K55G	100	83	98	22
N54A, K55S (Δ56-65)	14	—	22	—
K64A, R65S	103	76	98	—
K64A, R65S (Δ66-75)	—	—	—	—
L58A, R59G	34	36	55	—
K74A, E75S	CL:weak	CL:strong	83	—
N77A, K78S	105	98	87	—

[a] Relative activities of mutated proteins were standardized to 100% dimerization and RNA-binding efficiencies of wild-type SRP14. Standard deviations in the experimental approaches were between 10 and 20%.
[b] Truncated proteins that dimerize.
[c] Previously published without quantification in Bovia et al. (1994).
[d] Improved dimerization in presence of the RNA.
[e] Positive result in crosslinking experiments.
[f] Specific loss of RNA binding.

We also tested the RNA-binding activities of the SRP14 proteins with two altered amino acids (Fig. 1C) to investigate a possible role of the basic amino acids in RNA-binding. All SRP14 variants with two altered amino acids that dimerized efficiently in the presence of 7S-Alu RNA were also found to bind with similar efficiencies as the wild-type heterodimer to 7S-Alu RNA (Fig. 5B, lane 1; Table 2), and specific binding to the RNA was entirely dependent on the presence of SRP9 (results not shown). In particular, neither replacing amino acids K31/K32 nor R42/K43 alone interfered with RNA binding of the heterodimer. The partial loss in RNA binding observed for SRP14 (K31A, K32S, Δ33-43) is therefore due to changing all four of the basic amino acids and/or to removing additional amino acids within the 33-43 region of SRP14. The SRP14 variant with decreased dimerization efficiency, SRP14 (L58A, R59G), also had lower RNA-binding activities. Unlike for C-terminally truncated proteins, the dimerization defect of this protein could not be rescued by RNA, suggesting a possible role of these residues in RNA-binding.

Our analysis identified one altered SRP14 and two altered SRP9 proteins that had lost their RNA-binding activities partially, demonstrating that both proteins contribute to RNA binding. Hence, we examined whether the combination of two defective SRP9 and

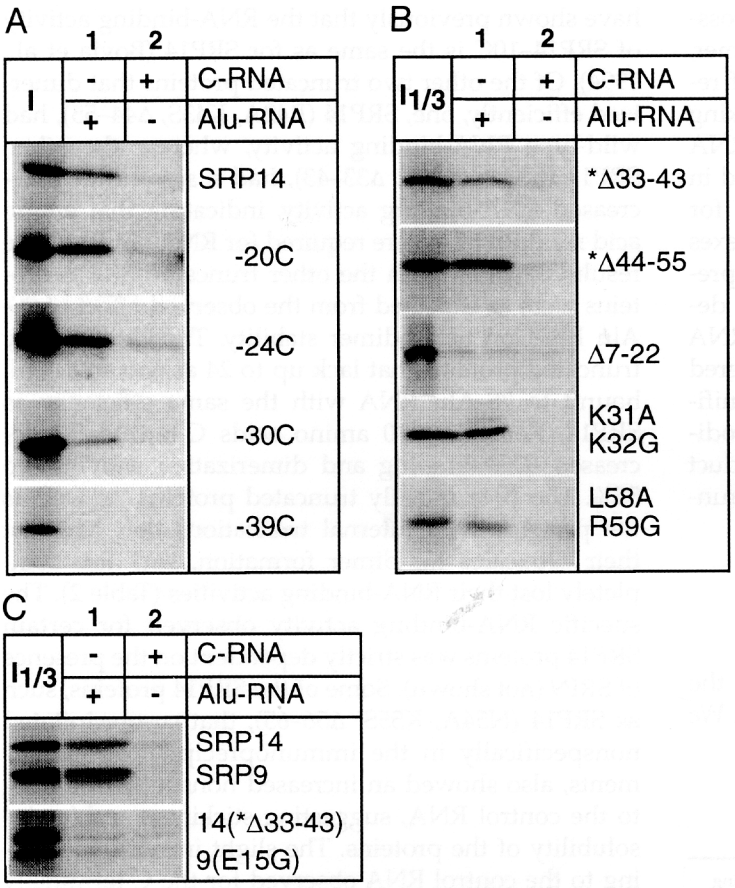

FIGURE 5. RNA-binding activities of altered SRP14 proteins. **A:** C-terminally truncated SRP14 proteins. **B:** SRP14 proteins with internal truncations. * indicates that the two amino acids preceding the truncations have been changed into A/S. **C:** RNA-binding activities of altered SRP9 and SRP14 proteins. Alu RNA, 7S-Alu RNA (lane 1). C-RNA, Control RNA (lane 2). I and $I_{1/3}$ represent all and 1/3 of the [^{35}S]-labeled protein used in the experiments, respectively.

SRP14 proteins resulted in a complete loss of specific RNA-binding activity. Both SRP14 (K31A, K32S, Δ33-43) and SRP9 (E15G) were synthesized in vitro and incubated with 7S-Alu RNA and the control RNA. As a positive control, we included in vitro-synthesized SRP9 and SRP14 in the analyses (Fig. 5C). As predicted from the previous results, the combination of two partially defective proteins leads to an almost complete loss of specific RNA-binding activity of the heterodimer. The wild-type proteins in the positive control bound 7S-Alu RNA efficiently.

SRP RNA facilitates assembly of dimerization-defective SRP14 proteins

An internal truncation in SRP14, SRP14 (Δ7–22), which removes the α1-helix (Fig. 1B), resulted in a complete loss of dimerization activity even in the presence of 7S-Alu RNA. The same truncation in SRP9 did not interfere with dimerization, but specifically abolished RNA-binding activity of the heterodimer. The high nonspecific co-precipitation of all N-terminally truncated proteins (Fig. 4B) suggested that their loss in activity may be due to misfolding of the protein. We decided to introduce more subtle changes into this region, hoping that they would not interfere with proper protein folding and would therefore allow us to distinguish between a defect in RNA-binding or dimerization. We produced SRP14 cDNAs in which highly conserved and/or basic N-terminal amino acids were changed into A/G (Fig. 6A). The different SRP14 proteins were analyzed in immunoprecipitation and crosslinking experiments as described before. Changing K19/C20 into A/G did not change the dimerization and RNA-binding activities of the protein (Fig. 6C). These two amino acid residues lie just outside the α1-helix of SRP14 (Fig. 1B). The other three mutated proteins, which contain substitutions within the α1-helix, failed to form a dimer with SRP9. However, they formed very stable complexes with 7S-Alu RNA comprising SRP14 and SRP9 proteins in close proximity to allow their crosslinking (Fig. 6B,C). Complex formation and the presence of SRP9 in these complexes was further confirmed by immunoprecipitation experiments with anti-myc antibodies (Fig. 6C). Thus, SRP RNA can engage dimerization-defective SRP14 proteins into RNA–protein complexes comprising both proteins. As expected from the dimerization experiments, the RNA-binding activities of all four proteins with two amino acid substitutions in the N-terminal portion of SRP14 were unchanged compared to SRP14 (Fig. 6C), confirming that these residues do not contribute directly to the RNA-binding activity of the heterodimer.

A

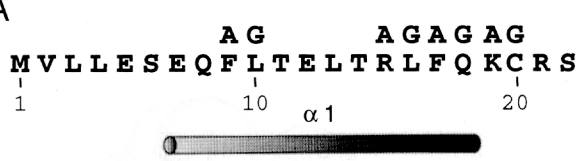

B

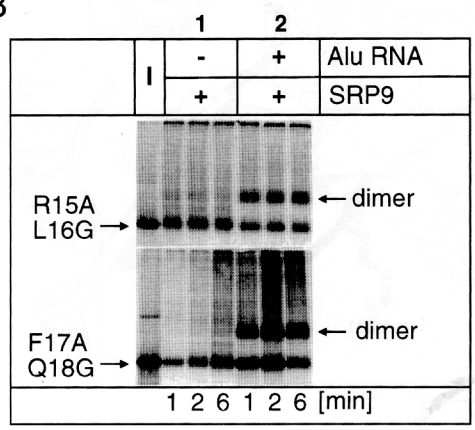

C

	SRP14 Proteins	Dimerization -Alu RNA	Dimerization +Alu RNA	RNA-binding Alu RNA	RNA-binding C RNA
■	F9A, L10G	- (-b)	113	78	16
■	R15A, L16G	- (-b)	78	97	10
■	F17A, Q18G	- (-b)	118	72	-
	K19A, C20G	105	115	122	-

FIGURE 6. Dimerization and RNA-binding activities of SRP14 proteins with mutations in the N-terminal region. **A:** Replaced amino acid residues in SRP14. **B:** Dimerization activities of the mutated [^{35}S]-labeled proteins assayed by crosslinking experiments in the absence (lane 1) and in the presence (lane 2) of 7S-Alu RNA. I, amount of protein used in the experiment. **C:** Quantification of the results. The activities of the mutated proteins were standardized to the activities of wild-type SRP14, which were set to 100%. ■ improved dimerization in presence of 7S-Alu RNA.

DISCUSSION

We undertook an extensive mutational analysis of the heterodimeric subunit SRP9/14 of murine SRP to identify regions that are required for the assembly of the heterodimer and for the formation of the complex with the Alu portion of SRP RNA. We found that the requirements for dimer formation are substantially different between the two proteins, despite their structural homology. In addition, structural elements from both proteins that lie in close proximity in the heterodimer contribute to the formation of an RNA-binding region.

The crystal structure of the heterodimer, which was determined in parallel (Birse et al., 1997), revealed that SRP9 and SRP14 are members of the family of small α/β RNA binding proteins, which includes ribosomal proteins (reviewed in Ramakrishnan et al., 1995), proteins containing the RNP domain (Oubridge et al., 1994a), the double-stranded RNA-binding domain (dsRBD, Bycroft et al., 1995; Kharrat et al., 1995), the KH domain (Musco et al., 1996), as well as the bacteriophage protein MS2 (Valegard et al., 1994) and the translation initiation factor IF3 (Biou et al., 1995). SRP9 and SRP14 are structurally homologous, folding into three β-strands flanked on each side by an α-helix. Together, they form a six-stranded antiparallel β-sheet stacked against the four α-helices with pseudo-twofold symmetry (Fig. 7A,B). The principal elements forming direct contacts are the β-strands β1 and the C-terminal helices α2 in both proteins, as well as the C-terminal region of SRP14 directly following α2. In particular, SRP14-K95 makes contacts with D54 and A56 in loop β3–α2 and SRP14-G93 with Y31 in the β1 strand of SRP9.

In agreement with the crystallographic studies, we found that removal of helix α1 in SRP9, such as in SRP9 (Δ6–17), does not interfere with its dimerization capacity. Somewhat unexpectedly, the removal of interface helix α2 completely, as in SRP9–30C, also fails to reduce the dimerization capacity of the protein. Hence, direct contacts between the β1 strands and the region following α2 in SRP14 are sufficient to produce a heterodimeric complex that is stable in immunoprecipitation experiments. This conclusion is supported by the finding that the internal portion of SRP9 comprising amino acid residues 23–56, thus lacking α1 and part of α2, preserves a low, but detectable capacity to form a heterodimer. In contrast, the removal of α1 and α2 completely, as in SRP9 (23–56), results in a complete loss of dimerization activity. Hence, α1 or α2 are interchangeably required for dimerization activity of SRP9, most likely because stacking of the α-helices against the three β-strands stabilizes the central β-strand region (Fig. 7A,B).

Unlike in SRP9 and in contrast to the apparent symmetry of the heterodimer, the ability to dimerize of SRP14 is radically diminished by all N-terminal truncations and by C-terminal truncations extending beyond 10 amino acids (except in the presence of 7S-Alu RNA). The loss in dimerization capacity is most likely explained by a lower stability or a reduced ability to fold of the truncated SRP14 proteins. This suggests that the α-helices have a more important structural role in SRP14 than in SRP9. This interpretation is consistent with the different topology of the two pairs of α-helices in the crystal structure of the heterodimer (Birse et al., 1997). The offset angle between the α-helices is smaller in SRP14 than in SRP9. In addition, the heterodimers comprising SRP14-20C and SRP14-30C proteins are further destabilized by the loss of interactions between the C-terminal amino acids 93–95 in SRP14 and SRP9. The dimerization defects of SRP14–20C and –30C could be rescued by the addition of SRP RNA, presumably because direct contacts between the RNA moiety and both proteins improved the stability of the complex.

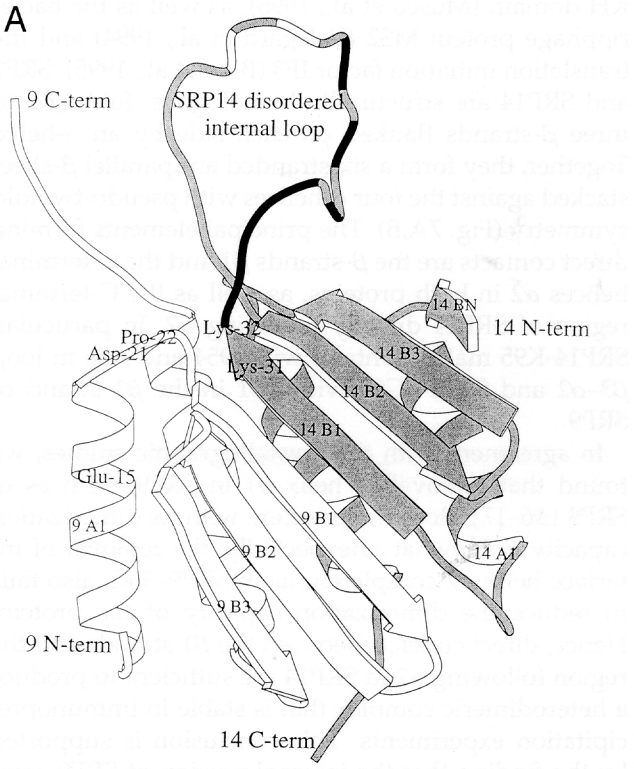

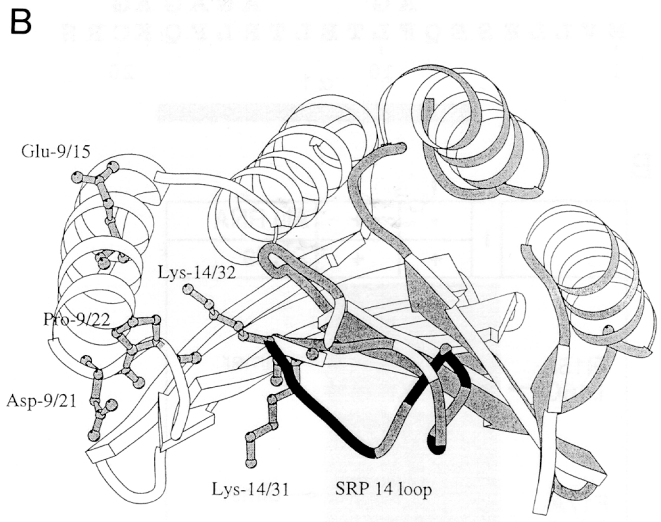

SRP9		SRP14	
		β_N	3-7
α_1	8-19	α_1	7-18
β_1	27-33	β_1	26-32
β_2	38-44	β_2	56-62
β_3	48-53	β_3	66-71
α_2	58-72	α_2	75-89

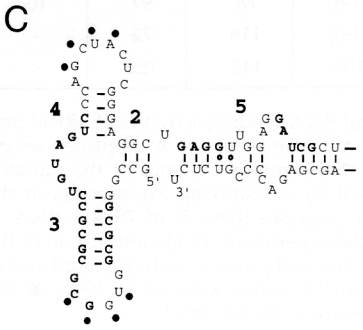

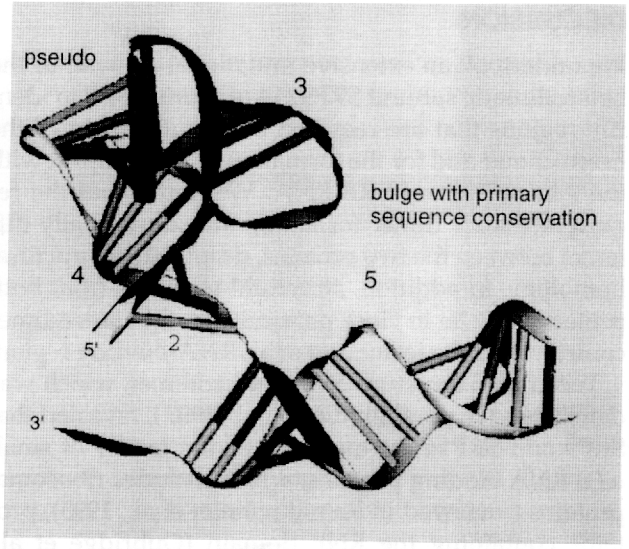

FIGURE 7. Protein and RNA structures of the Alu-domain. **A,B:** Two different views of the heterodimer SRP9/14. SRP14 and SRP9 are shown in gray and white, respectively. The boundaries of the secondary structure elements are shown in the inset. The disordered region in the large SRP14 loop is indicated in gray/white and black/white stripes. Upon deletion of the black and white loop region and the two preceding K residues in SRP14 (B), RNA-binding was diminished. Individual amino acid residues critical for RNA-binding in SRP9 are shown in B. **C,D:** The secondary structure and a model of the 3D structure of the SRP9/14 binding region in SRP RNA. The letters in bold (C) and regions in black (D) indicate the nucleotides that are protected from the attack of hydroxyl radicals in the presence of the heterodimer. The bulge between helices 3 and 4 is conserved in primary sequence (Strub et al., 1991). Black dots label the nucleotides forming the hypothetical pseudoknot structure in the 3D model of SRP RNA (Zwieb et al., 1996).

An important structural role of the α1-helix in SRP14, which is not part of the dimer interface, was further confirmed by mutations within this region that completely abolish the dimerization capacity of the protein. Yet, the addition of SRP RNA results in the formation of stable RNA–protein complexes comprising both proteins as a heterodimer. It is conceivable that low-affinity interactions between the RNA and SRP14 stabilize conformations or facilitate conformational changes in the protein that allow the assembly of the RNA–protein complex. Because these dimerization-deficient SRP14 proteins preserved their RNA-binding activities, it is likely that the same low-affinity interactions also occur with wild-type SRP14. So far, it has not been shown experimentally that the heterodimer represents an obligatory intermediate in the assembly of the RNA–protein complex in vivo. It was inferred from the stability of the heterodimeric complex (Strub & Walter, 1990) and from the observed co-regulation of SRP9 and SRP14 expression (Bovia et al., 1995). However, SRP9 and SRP14 recently have been suggested to play a role in the nucleo-cytoplasmic transport of SRP RNA (He et al., 1994). Thus, the assembly pathway of the Alu-domain may also be determined by factors other than the stability of the heterodimeric complex.

The regions in SRP14 dispensable for dimer formation include the 10 C-terminal amino acids and the large internal loop between β1 and β2 (shown black/white and gray/white in Fig. 7A,B). Both regions were found to be disordered in the crystal structure. In addition, the very basic C-terminal amino acid residues are also dispensable for SRP RNA-binding and for elongation arrest activity of the particle (Bovia et al., 1994).

We identified two regions, one in each protein, that are involved in RNA binding. The region in SRP9 comprises the N-terminal helix α1 and the adjacent loop linking α1 and β1 (Fig. 7A). Specifically, amino acid residues E15, as well as D21 and/or P22, were found to be critical for RNA binding. The side chains of residues E15, as well as D21, are exposed on the α-helical face of the heterodimer (Fig. 7B). An important role of acidic amino acid residues in contacting RNA has been recognized previously in ternary complexes of tRNAs and their cognate tRNA synthetases (Cavarelli et al., 1993; Cusack et al., 1996), as well as in the complex between the U1 RNA hairpin and the U1A protein (Oubridge et al., 1994b). Such residues may contact RNA via hydrogen bonds between amino groups of the base moieties in the RNA and the side-chain carboxyl group of the amino acid. Alternatively, their interaction with the RNA may possibly be mediated by magnesium ions. Replacing other amino acids, such as K16/L17 and E9/F10, resulted in a defect in the dimerization and RNA-binding functions (Table 1B). The dimerization efficiencies of both proteins could not be improved in the presence of Alu RNA, suggesting a role for these amino acid residues in RNA binding. Indeed, the partial loss of RNA-binding activity of SRP9 (E15) as compared to the complete loss in SRP9 (Δ6–17) is consistent with the removal of more than one RNA-binding determinant in the truncated protein.

The RNA-binding determinants that we have identified in SRP14 comprise the last two amino acids of β1 and the first half of the internal loop connecting the two β-strands, β1 and β2 (shown in black/white in Fig. 7A,B). The loop is disordered in the crystal and its structure is most likely determined by the interaction with the RNA. There is little primary sequence conservation in this region except for four basic residues K31, K32, R42, and K43 (Fig. 1). However, replacing two of the conserved basic residues at the same time fails to diminish the RNA-binding activity of the heterodimer, indicating that additional or other residues within the loop might be critical for RNA binding. Loop regions have also been found to be important RNA-binding determinants of other small α/β RNA-binding proteins, such as the ribosomal protein S5, the staufen protein of *Drosophila*, RNase III, and U1A protein (Nagai et al., 1990; Ramakrishnan & White, 1992; Bycroft et al., 1995; Kharrat et al., 1995). Aromatic and basic residues often seem to be involved in contacting RNA.

The RNA-binding determinants in the α1-helix and the adjacent loop of SRP9 lie in close proximity to the RNA-binding loop linking β1 and β2 of SRP14 in the heterodimer, consistent with the interpretation that together they form an RNA-binding region (Fig. 7B) required for high-affinity binding to the Alu-portion of mammalian SRP RNAs and to scAlu RNAs.

The three β-strands of SRP9 and SRP14 together form a concave β-sheet (Fig. 7B) with a highly positive charge due to a large number of exposed basic residues, suggesting that the β-sheet might serve as an RNA-binding surface (Birse et al., 1997). These exposed basic residues include K31, K55, R59, K66, and K74 in SRP14. The mutation of these residues has no noticeable effect on the RNA-binding capacities of the proteins (see Fig. 1; Table 2), except for the mutation R59G. SRP14 (L58A/R59G) has a decreased dimerization capacity that could not be improved by the addition of 7S-Alu RNA, consistent with a possible role of R59 in RNA-binding. Simultaneous mutation of several basic amino acid residues in SRP14 and/or the mutation of basic residues in SRP9 might be necessary to confirm a role of the positively charged β-sheet in RNA-binding. The fact that the heterodimer comprising SRP9 (Δ6–17) does not bind to SRP RNA indicates that the β-sheet surface alone is not sufficient for high-affinity binding of the RNA substrate. However, it is conceivable that it contributes to the formation of the very stable RNA–protein complex in addition to the RNA-binding determinants discussed before.

The regions in SRP RNA that are likely to contact the protein (Strub et al., 1991) are located along the central stem and in the first stem and loop structure and the following single-stranded region (bold and black in Fig. 7C,D, respectively). The primary sequence of the single-stranded region has been found to be highly conserved in SRP RNAs of all three kingdoms (Strub et al., 1991). The possibility of base pairing between the two loops of the two stem loop structures is conserved in evolution, suggesting that they form a pseudoknot (Larsen & Zwieb, 1991). According to a model of the 3D structure of SRP RNA, the putative pseudoknot structure would partially fold back, with the highly conserved single-stranded region U23–G27 reaching toward the central stem and thereby forming a pocket that may contact the protein on both sides (Fig. 7D; Zwieb et al., 1996). The positively charged β-sheet surface would most likely contact the double-stranded stem (Birse et al., 1997), whereas the α1-helix and the following loop in SRP9 might interact with the pseudoknot structure, possibly with the highly conserved single-stranded loop between the RNA helices 3 and 4. In this model, the asymmetric location of the RNA-binding determinants on the heterodimer, which itself is highly symmetric, would reflect the asymmetric structure of the RNA.

The ribosomal protein S6 requires the presence of S18 to bind specifically to ribosomal RNA (Held et al., 1974). In addition, it has been found that several dsRBD or KH modules are required for specific RNA binding of the *Drosophila* proteins staufen (Ferrandon et al., 1994) and Bic-C (Mahone et al., 1995). However, the mechanisms that lead to specific recognition of the RNA in these multimeric complexes have not yet been identified. The phage protein MS2 binds exclusively as a homodimer to the translational repressor site on the replicase mRNA. Its RNA-binding domain is composed of basic amino acid residues protruding from the β-sheet surface composed of five β-strands of each subunit (Peabody, 1993; Valegard et al., 1994). The homodimeric subunits have a slightly different conformation in the homodimer and the residues required for specific RNA-binding differ in both subunits (Peabody & Lim, 1996). Thus, homodimerization of the MS2 protein resembles heterodimerization of the structurally homologous SRP9 and SRP14 proteins in that both result in the formation of an RNA-binding domain that recognizes an asymmetric RNA structure with high specificity.

The structural homology between SRP9 and SRP14 suggests that they are derived from a common ancestor, possibly a ribosomal protein. Our studies on the two proteins revealed that their functional properties such as stability, the ability to fold, and their interactions with the RNA may have diverged significantly. This adaptation may have been necessary to improve the specificity of the RNA-binding function or may be related to other cellular functions, such as the co-regulation of their expression and the assembly of the particle in vivo.

MATERIALS AND METHODS

Mutagenesis of SRP9 and SRP14 proteins

N- and C-terminally truncated proteins were obtained by introducing new initiation and new stop codons at the appropriate positions in the murine SRP9 (accession no. X78305) and SRP14 (accession no. M29264) cDNAs using PCR. The deleted cDNAs were introduced into the plasmids SP65 and pGEM-4 (Promega). The cDNA encoding SRP9-22N was obtained by linearizing the pSm9-2 plasmid containing the SRP9 cDNA with *Ava* II and *Xba* I. For the synthesis of SRP14-39C and -44C, the SRP14 cDNA was linearized with *Sac* I and *Sau* 3A, respectively. SRP14 proteins with two amino acid residues substituted by alanine and serine were obtained by introducing an *Nhe* I restriction site at the desired position by PCR (McPherson et al., 1991). The cDNAs encoding the N-terminal and the C-terminal portions of the altered SRP14 proteins were amplified separately and the PCR products were digested with *Eco*R I/*Nhe* I and with *Nhe* I (Melton et al., 1984) for the 5′ and 3′ fragments, respectively. The amplification products were combined subsequently and ligated into the linearized pGEM-4 plasmid to yield cDNAs encoding either proteins with two amino acid substitution or proteins with two amino acid substitutions and internal truncations. Some proteins with internal truncations, SRP9 (Δ6–17) and SRP14 (Δ7–22), and the proteins with two amino acids substituted for alanine and glycine were produced using either a two-step PCR mutagenesis approach, the megaprimer method (Sarkar & Sommer, 1990), or the QuickChange site-directed mutagenesis protocol of Stratagene. A novel Cfr10I restriction enzyme site was created at the position of the mutation. The sequences of all newly created cDNAs were confirmed by dideoxy sequencing.

In vitro transcription and translation

RNAs were synthesized from the various linearized plasmids using SP6 or T7 RNA polymerase (Melton et al., 1984). The proteins were synthesized in wheat germ extract in the presence of [^{35}S]-labeled methionine (Amersham Corp. 1,500 Ci/mmol), as described in Strub and Walter (1990). For all mutated cDNAs we analyzed, we observed a single major [^{35}S]-labeled translation product that migrated in SDS-PAGE, as expected from the predicted molecular weight of the truncated protein.

Overexpression and purification of SRP9 and SRP14 proteins in bacteria

Murine SRP9 was expressed and purified as described in Strub et al. (1993). The proteins SRP14m and SRP9m comprise 12 additional amino acids at their C termini. The short peptide, GGEQKLISEEDL, constitutes a well-defined epitope recognized by anti-myc antibodies (Evan et al., 1985). The sequences encoding the myc epitope, as well as an *Nde* I restriction site at the initiator methionine were added to the

coding regions of SRP9 and SRP14 using PCR. The resulting SRP9m and SRP14m cDNAs were inserted into the pET3b expression vector (Studier et al., 1990). The expression level of murine SRP14 is very low in bacteria, presumably because of its instability. The addition of the myc epitope to its C terminus improves the expression of the protein to a level sufficiently high for its subsequent purification. Transformed BL21(DE3) bacteria (500 mL) were grown to an optical density A_{600} = 0.6 and protein synthesis was induced with 0.8 mM isopropyl-β-D-thiogalactopyranoside during 3 h. Cells were lysed as described previously (Bovia et al., 1994). Both proteins were purified on 10 mL heparine and 10 mL CM columns (Bio-Rad). No other proteins were detectable in the purified SRP9m protein sample, whereas SRP14cm was enriched to about 80% after the two-step procedure. The proteins were quantified by comparing to a Coomassie-stained lysozyme standard. The SRP14 cDNA (Strub & Walter, 1989) was ligated into pGEX-3X vector linearized with *Eco*R I for the expression of the glutathione-S-transferase-SRP14 fusion protein (G-14). The glutathione-S-transferase (GST) was expressed directly from pGEX-3X. The proteins G-14 and GST were produced in DH5α cells and purified as described (Smith & Johnson, 1988; New England Biolabs protocol). Their concentration was determined by comparing to a Coomassie-stained standard of γ-globulin.

Dimer formation experiments

For the immunoprecipitation experiments, the [^{35}S]-labeled SRP14 proteins were incubated with a 10-fold excess of recombinant SRP9m in the presence or absence of a 20-fold excess of 7S-Alu RNA in a final volume of 20 μL IPW buffer (50 mM Tris-HCl, pH 7.5, 350 mM potassium acetate, 0.1% Triton X-100, 0.01% Nikkol) for 10 min at 0 °C and 10 min at 37 °C. The binding reaction was diluted with 20 μL IPW buffer containing 1× protease inhibitors (200× stock solution contains 20 μg/mL each of pepstatin A, leupeptin, antipain, chymostatin, and 100 μg/mL of aprotinine) and added to 20 μL protein G beads (Pharmacia) loaded with goat anti-mouse and with monoclonal 9E10 anti-myc antibodies (Evan et al., 1985). The myc epitope in SRP9 was well recognized by the antibodies in the protein and in the protein-RNA complex, and it did not interfere with binding of the heterodimer to 7S-Alu RNA (results not shown). For co-immunoprecipitation of [S^{35}]-labeled SRP9 proteins, we used a 10-fold excess of SRP14m, together with affinity-purified anti-SRP14 antibodies (Bovia et al., 1995) and protein A beads (Pharmacia). Binding was allowed to continue for 60 min by rotating the tubes at 4 °C end over. The beads were pelleted for 30 s in a microfuge at 4,000 rpm, the supernatants removed, and the beads were washed three times with 300 μL IPW buffer by rotating end over for 3 min. Alternatively, the [S^{35}]-labeled SRP9 proteins were incubated with glutathione-Sepharose beads loaded with G-14 or with GST proteins, in the presence and in the absence of a 20-fold excess of 7S-Alu RNA in binding buffer (50 mM Tris-HCl, pH 7.5, 350 mM potassium acetate, 3.5 mM magnesium acetate, 0.01% Nikkol, 0.1% Triton X-100). The samples were incubated for 10 min at 4 °C, for 10 min at 37 °C, and for 45 min at 4 °C by rotating the tubes end over. The beads were washed as described for the immunoprecipitation experiments. The bound SRP14 proteins were displayed by 17% SDS-PAGE and the SRP9 proteins by Tricine gel electrophoresis (Schägger & Von Jagow, 1987). Crosslinking reactions were performed exactly as described (Bovia et al., 1994). Briefly, the [S^{35}]-labeled SRP14 proteins (80 μL translation reactions) were purified on heparin gel (Bio-Rad). The eluted proteins were incubated with 20 pmol of SRP9 recombinant protein, and either with or without 20 pmol SRP RNA for 10 min at 0 °C and for 10 min at 37 °C. The protein samples were split and glutaraldehyde was added at a final concentration of 0.08%. The crosslinking reactions were stopped at 1, 2, and 6 min with 0.1 M Tris buffer. Time point 0 (input) was obtained by adding Tris buffer before adding the glutaraldehyde. The protein samples were analyzed by 17% SDS-PAGE. The autoradiographs were scanned and the results quantified using the Scan Analysis program (v. 2.50, Biosoft). Co-precipitation efficiencies were 40 ± 5% with the polyclonal affinity-purified antibodies, 26 ± 3% with the G-14 protein and 22 ± 3% with the anti-myc antibodies. Dimerization efficiencies of SRP14 and of SRP9 were set to 100% for the calculation of the relative dimerization efficiencies of the altered proteins. The relative standard deviation in all experimental approaches was 10–15%.

RNA-binding experiment

7S-Alu and the control RNA were synthesized from the plasmids p7Salu (Strub et al., 1991) and pG14-2 (Strub & Walter, 1989) using T7 RNA polymerase and 1 mM and 100 μM of each nucleotide triphosphate and of biotinylated UTP, respectively (Milligan et al., 1987). The control RNA represents a 368-nt transcript from the antisense strand of the SRP14 cDNA. The streptavidin binding was described previously (Bovia et al., 1994). Briefly, the [S^{35}]-labeled SRP9 or SRP14 proteins were incubated with or without a 20-fold excess of recombinant SRP9 or SRP14 proteins and with either a 20-fold excess of biotinylated Alu RNA or biotinylated control RNA. Competitor RNA (1 μg of *Escherichia coli* tRNA) and protease inhibitors (see above) were also added to the binding reaction, which was in 350 mM potassium acetate. After incubation for 10 min at 0 °C and 10 min at 37 °C, the RNA-bound proteins were collected by a quick centrifugation of the streptavidin beads (Böhringer Mannheim, Enzo diagnostics Inc). The RNA-bound proteins were analyzed after three washes of 3 min by 17% SDS-PAGE (SRP14) or by Tricine gel electrophoresis (SRP9). The autoradiographs were scanned and the results quantified using the Scan Analysis program. The RNA-binding efficiency for SRP9/14 was 38 ± 5% and was set to 100% for the calculation of the relative binding efficiencies of the altered proteins.

ACKNOWLEDGMENTS

We thank Didier Picard for critical reading of the manuscript, Christian Zwieb for Figure 7D, and Monique Fornallaz for technical assistance. This work was supported by a grant from the Swiss National Science Foundation and the Canton de Genève. K.S. is a fellow of the START program of the Swiss National Science Foundation. K.S. and S.C. are both members of SRPNET, which is supported under the European Union Training and Mobility of Researchers program and by the Swiss Government.

Received March 12, 1997; returned for revision March 25, 1997; revised manuscript received April 7, 1997

REFERENCES

Althoff S, Selinger D, Wise JA. 1994. Molecular evolution of SRP cycle components: Functional implications. *Nucleic Acids Res 22*:1933–1947.

Bacher G, Lütcke H, Jungnickel B, Rapoport TA, Dobberstein B. 1996. Regulation by the ribosome of the GTPase of the signal-recognition particle during protein targeting (see comments). *Nature 381*:248–251.

Biou V, Shu F, Ramakrishnan V. 1995. X-ray crystallography shows that translational initiation factor IF3 consists of two compact alpha/beta domains linked by an alpha-helix. *EMBO J 14*:4056–4064.

Birse DEA, Kapp U, Strub K, Cusack S, Åberg A. 1997. The crystal structure of the signal recognition particle *Alu* RNA binding heterodimer, SRP9/14. *EMBO J.* Forthcoming.

Bovia F, Bui N, Strub K. 1994. The heterodimeric subunit SRP9/14 of the signal recognition particle functions as permuted single polypeptide chain. *Nucleic Acids Res 22*:2028–2035.

Bovia F, Fornallaz M, Leffers H, Strub K. 1995. The SRP9/14 subunit of the signal recognition particle (SRP) is present in more than 20-fold excess over SRP in primate cells and exists primarily free but also in complex with small cytoplasmic Alu RNAs. *Mol Biol Cell 6*:471–484.

Bovia F, Strub K. 1996. The signal recognition particle and related small cytoplasmic ribonucleoprotein particles. *J Cell Sci 109*:2601–2608.

Bovia F, Wolff N, Ryser S, Strub K. 1997. The SRP9/14 subunit of the human signal recognition particle binds to a variety of Alu-like RNAs and with higher affinity than its mouse homolog. *Nucleic Acids Res 25*:318–325.

Bycroft M, Grunert S, Murzin AG, Proctor M, St Johnston D. 1995. NMR solution structure of a dsRNA binding domain from *Drosophila* staufen protein reveals homology to the N-terminal domain of ribosomal protein S5. *EMBO J 14*:3563–3571.

Cavarelli J, Rees B, Ruff M, Thierry JC, Moras D. 1993. Yeast $tRNA^{asp}$ recognition by its cognate class II aminoacyl-tRNA synthetase. *Nature 362*:181–184.

Chang DY, Maraia RJ. 1993. A cellular protein binds B1 and Alu small cytoplasmic RNAs in vitro. *J Biol Chem 268*:6423–6428.

Chang DY, Nelson B, Bilyeu T, Hsu K, Darlington G, Maraia RJ. 1994. A human Alu RNA-binding protein whose expression is associated with accumulation of small cytoplasmic Alu RNA. *Mol Cell Biol 14*:3949–3959.

Cusack S, Yaremchuk A, Tukalo M. 1996. The crystal structure of the ternary complex of *T. thermophilus* seryl-tRNA synthetase with $tRNA^{ser}$ and a seryl-adenylate analogue reveals a conformational switch in the active site. *EMBO J 15*:2834–2842.

Evan GI, Lewis GK, Ramsay G, Bishop JM. 1985. Isolation of monoclonal antibodies specific for human c-myc proto-oncogene product. *Mol Cell Biol 5*:3610–3616.

Ferrandon D, Elphick L, Nusslein-Volhard C, St Johnston D. 1994. Staufen protein associates with the 3'UTR of bicoid mRNA to form particles that move in a microtubule-dependent manner. *Cell 79*:1221–1232.

Hann BC, Poritz MA, Walter P. 1989. *Saccharomyces cerevisiae* and *Schizosaccharomyces pombe* contain a homologue to the 54-kD subunit of the signal recognition particle that in *S. cerevisiae* is essential for growth. *J Cell Biol 109*:3223–3230.

Hauser S, Bacher G, Dobberstein B, Lutcke H. 1995. A complex of the signal sequence binding protein and the SRP RNA promotes translocation of nascent proteins. *EMBO J 14*:5485–5493.

He XP, Bataille N, Fried HM. 1994. Nuclear export of signal recognition particle RNA is a facilitated process that involves the Alu sequence domain. *J Cell Sci 107*:903–912.

Held WA, Ballou B, Mizushima S, Nomura M. 1974. Assembly mapping of 30S ribosomal proteins from *Escherichia coli*. *J Biol Chem 249*:3103–3111.

Janiak F, Walter P, Johnson AE. 1992. Fluorescence-detected assembly of the signal recognition particle: Binding of the two SRP protein heterodimers to SRP RNA is noncooperative. *Biochemistry 31*:5830–5840.

Kharrat, A, Macias MJ, Gibson TJ, Nilges M, Pastore A. 1995. Structure of the dsRNA binding domain of *E. coli* RNase III. *EMBO J 14*:3572–3584.

Larsen N, Zwieb C. 1991. SRP-RNA sequence alignment and secondary structure. *Nucleic Acids Res 19*:209–215.

Luirink J, High S, Wood H, Giner A, Tollervey D, Dobberstein B. 1992. Signal-sequence recognition by an *Escherichia coli* ribonucleoprotein. *Nature 359*:741–743.

Lütcke H. 1995. Signal recognition particle (SRP), a ubiquitous initiator of protein translocation. *Eur J Biochem 228*:531–550.

Mahone M, Saffman EE, Lasko PF. 1995. Localized bicaudal-C RNA encodes a protein containing a KH domain, the RNA binding motif of FMR1. *EMBO J 14*:2043–2055.

Melton DA, Krieg PA, Rebagliati MR, Maniatis T, Zinn K, Green MR. 1984. Efficient in vitro synthesis of biologically active RNA and RNA hybridization probes from plasmids containing a bacteriophage SP6 promoter. *Nucleic Acids Res 12*:7035–7056.

Miller JD, Wilhelm H, Gierasch L, Gilmore R, Walter P. 1993. GTP binding and hydrolysis by the signal recognition particle during initiation of protein translocation. *Nature 366*:351–354.

Milligan JF, Groebe DR, Witherell GW, Uhlenbeck OC. 1987. Oligoribonucleotide synthesis using T7 RNA polymerase and synthetic DNA templates. *Nucleic Acids Res 15*:8783–8798.

Musco G, Stier G, Joseph C, Castiglione Morelli MA, Nilges M, Gibson TJ, Pastore A. 1996. Three-dimensional structure and stability of the KH domain: Molecular insights into the fragile X syndrome. *Cell 85*:237–245.

Nagai K, Oubridge C, Jessen TH, Li J, Evans PR. 1990. Crystal structure of the RNA-binding domain of the U1 small nuclear ribonucleoprotein A [see comments]. *Nature 348*:515–520.

Oubridge C, Ito N, Evans PR, Teo CH, Nagai K. 1994a. Crystal structure at 1.92 Å resolution of the RNA-binding domain of the U1A spliceosomal protein complexed with an RNA hairpin. *Nature 372*:432–438.

Oubridge C, Nobutoshi I, Evans PR, Teo CH, Nagai K. 1994b. Crystal structure at 1.92 Å resolution of the RNA-binding domain of the U1A spliceosomal protein complexed with an RNA hairpin. *Nature 372*:432–438.

Peabody DS. 1993. The RNA binding site of bacteriophage MS2 coat protein. *EMBO J 12*:595–600.

Peabody DS, Lim F. 1996. Complementation of RNA binding site mutations in MS2 coat protein heterodimers. *Nucleic Acids Res 24*:2352–2359.

Phillips GJ, Silhavy TJ. 1992. The *E. coli* ffh gene is necessary for viability and efficient protein transport. *Nature 359*:744–746.

Ramakrishnan V, Davies C, Gerchman SE, Golden BL, Hoffmann DW, Jaishree TN, Kyila JH, Porter S, White SW. 1995. Structures of prokaryotic ribosomal proteins: Implications for RNA binding and evolution. *Biochem Cell Biol 73*:979–986.

Ramakrishnan V, White SW. 1992. The structure of ribosomal protein S5 reveals sites of interaction with 16S rRNA. *Nature 358*:768–771.

Rapiejko P, Gilmore R. 1992. Protein translocation across the ER requires a functional GTP binding site in the α-subunit of the signal recognition particle receptor. *J Cell Biol 117*:493–503.

Sarkar G, Sommer SS. 1990. The megaprimer method of site directed mutagenesis. *BioTechniques 8*:404–407.

Schägger H, Von Jagow G. 1987. Tricine-sodium dodecyl sulfate-polyacrylamide gel electrophoresis for the separation of proteins in the range from 1 to 100 kDa. *Anal Biochem 166*:368–379.

Siegel V, Walter P. 1986. Removal of the Alu structural domain from signal recognition particle leaves its protein translocation activity intact. *Nature 320*:81–84.

Smith DB, Johnson KS. 1988. Single-step purification of polypeptides expressed in *Escherichia coli* as fusions with glutathione-S-transferase. *Gene 67*:31–40.

Strub K, Moss J, Walter P. 1991. Binding sites of the 9- and 14-kilodalton heterodimeric protein subunit of the signal recognition particle (SRP) are contained exclusively in the Alu domain of SRP RNA and contain a sequence motif that is conserved in evolution. *Mol Cell Biol 11*:3949–3959.

Strub K, Walter P. 1989. Isolation of a cDNA clone of the 14-kDa subunit of the signal recognition particle by cross-hybridization

of differently primed polymerase chain reactions. *Proc Natl Acad Sci USA 86*:9747–9751.

Strub K, Walter P. 1990. Assembly of the Alu domain of the signal recognition particle (SRP): Dimerization of the two protein components is required for efficient binding of SRP RNA. *Mol Cell Biol 10*:777–784.

Strub K, Wolff N, Oertle S. 1993. The Alu-domain of the signal recognition particle. In: Nierhaus KH, Franceschi F, Subramanian AR, Erdmann VA, Wittmann-Liebold B, ed. *The translational apparatus*. New York: Plenum Press. pp 635–645.

Studier FW, Rosenberg AH, Dunn JJ, Dubendorff JW. 1990. Use of T7 RNA polymerase to direct expression of cloned genes. *Methods Enzymol 185*:60–89.

Ullu E, Tschudi C. 1984. Alu sequences are processed 7SL RNA genes. *Nature 312*:171–172.

Valegard K, Murray JB, Stockley PG, Stonehouse NJ, Liljas L. 1994. Crystal structure of an RNA bacteriophage coat protein–operator complex. *Nature 371*:623–626.

Walter P, Johnson AE. 1994. Signal sequence recognition and protein targeting to the endoplasmic reticulum membrane. *Annu Rev Cell Biol 10*:87–119.

Wilson R et al. (1994). 2.2 Mb of contiguous nucleotide sequence from chromosome III of *C. elegans*. *Nature 368*:32–38.

Wolin SL. 1994. From the elephant to *E. coli*: SRP dependent protein targeting. *Cell 77*:787–790.

Zwieb C, Müller F, Larsen N. 1996. Model of the 3D structure of human SRP RNA. *Folding & Design 1*:315–324.